MHD Simulations for Studies of Disruption Mitigation by High Pressure Noble Gas Injection

V.A. Izzo 1), R.S. Granetz 1), D.G. Whyte 1), M. Bakhtiari 2)
1) MIT Plasma Science and Fusion Center, Cambridge, MA, USA
2) University of Wisconsin, Madison, WI, USA

e-mail contact: izzo@psfc.mit.edu

The problem of disruptions is a major challenge for ITER which establishes engineering and operational limits. MHD simulations including radiation and atomic physics have the capability of extending results of mitigation experiments on present devices to accurate predictions for ITER. The role of MHD in cases where impurity penetration is shallow is seen in a series of Alcator C-Mod simulations employing a simple radiation model to cool the tokamak edge with an assumed penetration between 1.5 and 3.0 cm. Results indicate that this shallow penetration is sufficient to trigger a core thermal quench, and predict a relationship between the delay before the quench onset and the separation between the cooling front and the q = 2 surface. This prediction can be tested experimentally by varying the effective penetration relative to q = 2. The simulations qualitatively reproduce several features of a gas-jet induced thermal quench on C-Mod, but a more sophisticated model is required for a truly predictive code that can be extended to ITER. Improved modeling of the impurities is achieved through the coupling of the 3D NIMROD MHD code and the 0D KPRAD radiation code, to obtain accurate radiation rates and track all charge state populations. Simulations for several gas species are possible. Preliminary results from the new code are presented, and comparison is made with C-Mod bolometry data.

1. Introduction

Considerable fears of structural damage caused by discharge terminating disruptions in large tokamaks like ITER have prompted substantial experimental research into strategies to mitigate harmful effects, assuming disruptions can not be avoided altogether. Three negative consequences of disruptions must be mitigated. Namely, 1) halo currents flowing poloidally in the divertor, generating large stresses, 2) deposition of large heat loads on the divertor causing melting or ablation of divertor material, and 3) production of runaway electrons which eventually impact the plasma facing components. Potentially, each of these effects can be mitigated by the injection of a high-pressure jet of noble gas when a disruptive event begins. The gas allows a significant fraction of the energy to be lost in the form of isotropic radiation, while an increase in electron density and loss of core confinement may prevent runaway electron production. Successful gas-jet mitigation experiments have been performed on several tokamaks, including DIII-D[1,2,3] and Alcator C-Mod.[4] The C-Mod experiments and those in Ref. [3] on DIII-D indicate only shallow penetration of the jet beyond the separatrix, yet a rapid core thermal quench ensues. Simple radiation by a uniformly deposited jet clearly does not model the gas-jet induced thermal quench, in which MHD instabilities are seen to play an important role. MHD can potentially hasten the thermal quench by two means, either by mixing impurity ions into the core, or by creating stochastic field lines, along which heat flows rapidly to the region of high impurity density. The interaction between gas-jet induced radiation and MHD instabilities can be better understood with the aid of MHD simulations. Such simulations may also supply the predictive capability needed to test mitigation strategies for ITER.

2. NIMROD Simulations

A high-pressure gas jet has the initial effect of cooling plasma just inside the tokamak separatrix in a relatively short time. The effects of this rapid cooling on an Alcator C-Mod equilibrium were studied in a series of MHD simulations with the NIMROD code.[5] The code evolves density, magnetic field, velocity, and temperature, with $T_e=T_i$ assumed and anisotropic thermal conduction ($k_{\|}=10^8 m^2 s^{-1}$ and $k_{\perp}=1\ m^2 s^{-1}$). The resistivity is enhanced by factor of ~100 above C-Mod experimental values to reduce computational expense. The simulated Lunquist number is $S=2\cdot10^5$. The resistivity is also temperature dependent according to the Spitzer model ($\sim T^{-3/2}$).

Additionally, a simple radiation model is included in the code to cool a region extending a fixed, specified distance inside the separatrix. The cooling occurs uniformly in the toroidal and poloidal directions. For convenience, the coronal equilibrium (CE) cooling coefficients for argon are used, with argon assumed to be present in a fixed fraction everywhere outside the assumed jet penetration radius. The CE approximation is not expected to be accurate on the short time scales involved, but is merely included to produce the expected rapid cooling. A different jet penetration radius, δ_z, ranging from 1.5-3 cm at the midplane is chosen in each of four simulations.

Results from these four simulations clearly show that a more rapid thermal quench occurs as the assumed impurity penetration depth is increased. This can be seen in FIG. 1, in which total thermal energy vs. time is plotted for each case. The q=2 surface for this equilibrium is approximately 2.5 cm from the separatrix at the midplane. A clear division is seen between those cases in which the q=2 surface is cooled directly by the impurity model and those in which the penetration is more shallow.

An m=2/n=1 mode is initially dominant in each simulation. This is consistent with magnetic fluctuations observed in DIII-D experiments.[3] The growth rate of the 2/1 mode is dependent on the jet penetration depth, and is notably larger in the δ_z=2.5 and 3.0 cm cases. In those cases the cooling at the q=2 surface increases the resistivity at that location and consequently the growth rates. The initial n=1 growth rate for the four simulations is seen in FIG. 2.

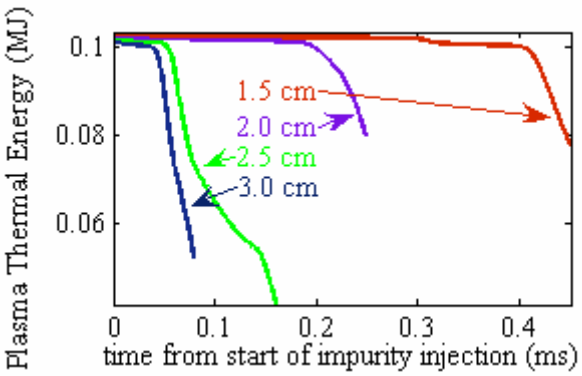

FIG. 1. Plasma thermal energy vs. time

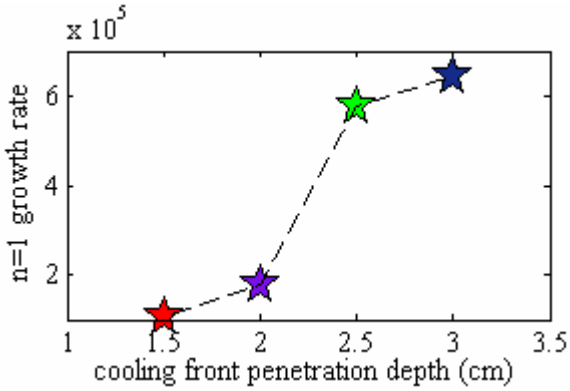

FIG. 2. Initial n=1 growth rate vs. jet penetration radius

The 2/1 mode becomes large, and, in conjunction with higher n modes, eventually destroys all of the flux surfaces outside of the q=1 surface. In the latter stage of the thermal quench, an m=1/n=1 mode becomes important, as the hot tokamak core is swapped with a cooler 1/1 island. The process by which heat escapes from the plasma and is radiated at the edge is seen in a series of puncture plots in FIG. 3 with temperature superimposed. The cooling of the region outside of q=1 occurs once the fields in that region become stochastic, while the 1/1 mode expels most of the heat from the core. However, a significant region of closed flux remains at the end of the simulations.

Temperature profiles from the simulations can be compared directly with Thomson scattering profiles taken during gas jet disruption experiments on C-Mod. Experimentally, limitations on the minimum spacing of the Thomson profiles in time necessitate taking a series of profiles over successive repeatable shots in order to map the temperature evolution. Shown in FIG. 4 are a series of profiles for a C-Mod experiment using a krypton gas jet, as well a set of 1D profiles from the same simulation as FIG. 3. In each case the target profile is shown along with three profiles taken once the gas jet begins to interact with the plasma. These latter three profiles are spaced evenly in time in each case, but the simulated profiles are spaced by 20μs while the experimental profiles are 400μs apart. Enhanced MHD growth rates are associated with the reduced Lundquist number of the simulations, with an expected scaling of $\sim S^{-0.6}$. Therefore, approximately a factor of 20 difference in time scale is expected for an S ratio of 100.

Despite different initial temperatures and different MHD time scales, the qualitative features of the experimental and simulated thermal quenches are quite consistent. In each case, the outer few cm are initially cooled directly by the gas jet. Next, the outer ~40% of the minor radius begins to cool, which is due to the formation of stochastic fields in the simulations. Finally, the rapid flattening of the core temperature profile associated with the 1/1 mode occurs. Significant reheating at r/a>0.6 is observed in both experiment and simulation as the core heat is ejected. The thermal quench in C-Mod experiments occurs too quickly to diagnose magnetic fluctuations directly. This comparison of temperature profile evolution is the best evidence to support the

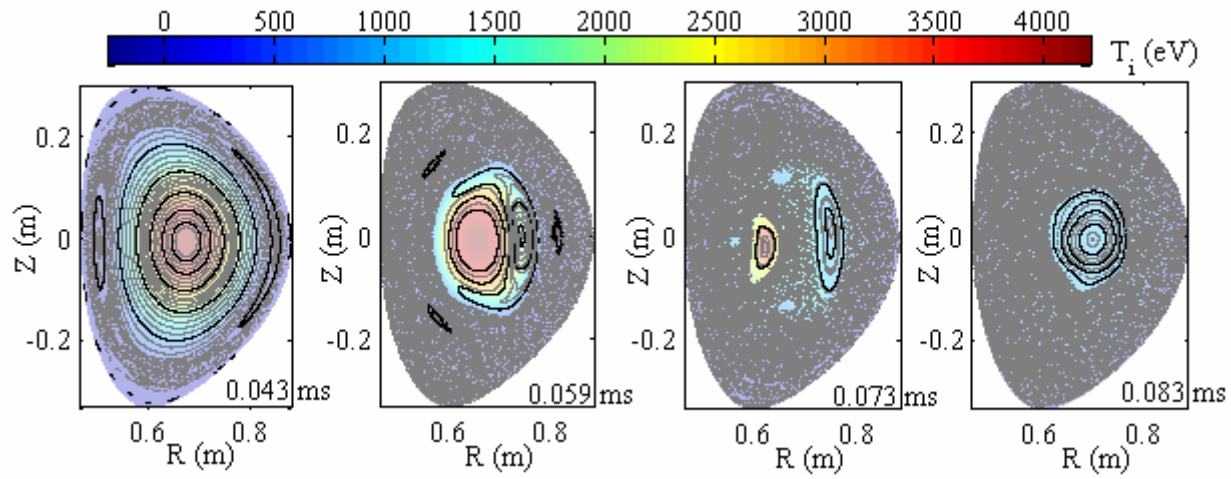

FIG. 3. Puncture plot of magnetic field lines in the δ_z = 3.0 cm simulation at four times. Temperature contours are superimposed.

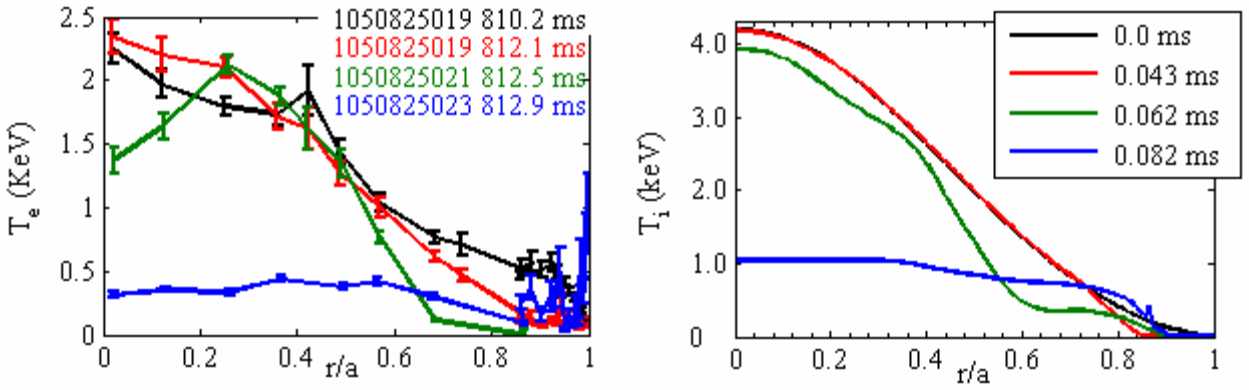

FIG. 4. (left) Thomson scattering profiles for a series of repeatable C-Mod discharges with an krypton gas jet fired at 800 ms. (right) Sequence of temperature profiles for the δ_z=3.0 cm NIMROD simulation.

belief that a sequence of MHD events very similar to those in the simulation is occurring during these C-Mod discharges. The observed similarities despite the assumed, fixed impurity penetration assumption suggests a large role for heat transport along stochastic fields, as opposed to impurity mixing to the core in the C-Mod experiments.

For 1.5-2.0 cm gas jet penetration, a significant delay is observed between the cooling of the edge and the onset of the thermal quench, with more than twice the delay for 1.5 cm than for 2.0 cm (FIG. 1). This difference is not accounted for by the difference in n=1 growth rate, which is less than a factor of 2 (FIG. 2). Rather, the thermal quench onset in the shallow penetration cases coincides with the eventual intersection of the 2/1 island with radiating edge region. A greater distance between the q=2 surface and the gas jet cold front delays this event. In FIG. 5 profiles of the edge temperature for the 2.0 cm simulation are shown. The intersection of the island with the cold front is evidenced by the appearance of a temperature dip on the low minor radius side of the island. The initial appearance of stochastic fields coincides with this intersection, as does the start of the thermal quench, as seen by comparison with FIG 1. These results suggest that q-profile could play a role in the timing of a gas-jet induced thermal quench, if indeed the jet is stopped just inside the separatrix.

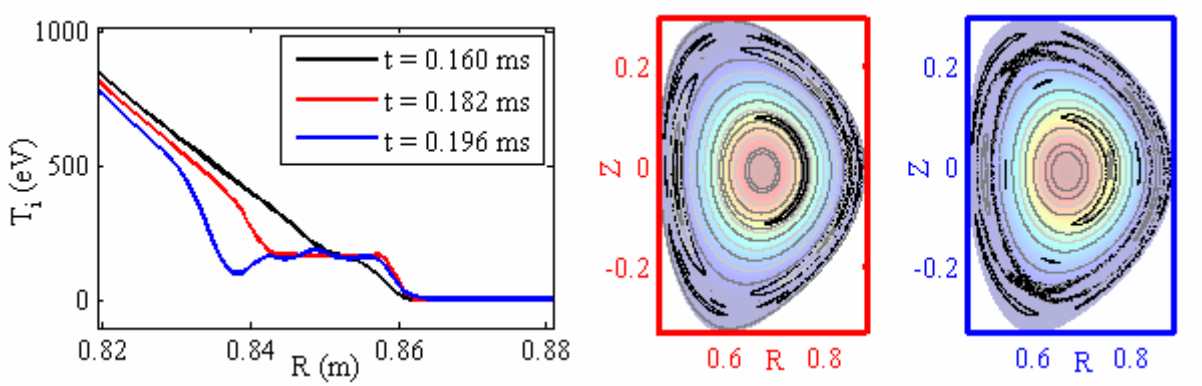

FIG. 5. (left) Edge temperature profiles for the δ_z=2.0 cm simulation. The blue profile is just after the intersection of the 2/1 island with the cold-front. (right) Field line puncture plots at the times of the red and blue temperature profiles, respectively.

3. NIMROD + KPRAD

The preceding simulations are a useful tool for better understanding experimental results, but can not be considered predictive. Nor do these results explain all observations from Alcator C-Mod experiments. For instance, large core density increases are seen during a helium jet induced disruption, but not for higher Z gas jets. Better understanding of the role of impurity mixing or any of the variations observed between gas species will require a much more sophisticated gas jet model. Also, accurate radiation rates will be required to simulate the competition between radiation and heat transport near the boundary, which determines heat flux across the separatrix and ultimately to the divertor. Finally, the most reliable extrapolation of a gas jet mitigation strategy to ITER can be accomplished with a predictive, first-principles code that has been benchmarked against one or more existing tokamaks.

With these aims, the KPRAD[6] atomic physics code has been incorporated into NIMROD to allow the accurate calculation of ionization, recombination and radiation rates with no equilibrium assumption. This necessitates tracking all charge states for the given impurity species. Additionally, a gas dynamic code separately calculates the gas flow down the injection tube, giving total gas injection rate versus time. The gas jet penetration is based on the ablation pressure model of Parks,[7] in which the incoming jet pressure competes with the ablation pressure at the front of the jet, which depends on density and temperature approximately as $n_e^{2/3}T_e^{5/3}$. Presently, this ablation pressure is calculated for an entire flux surface. The neutral gas is deposited uniformly in the poloidal and toroidal directions outside the penetration radius. Note that due to the weaker dependence on density, the ablation pressure of a flux surface will decrease even due to adiabatic cooling, causing the penetration radius to move inward with time, but a stronger radiator will more quickly push its way into the plasma.

The combined NIMROD/KPRAD code, henceforth referred to as NIMRAD, contains additional terms or modifications to each of the NIMROD equations. In the continuity equation, a source/sink term is included to account for ionization/recombination of impurities as well as deuterium 3-body recombination, which becomes relevant at sub-1eV temperatures.

$$\frac{dn_e}{dt} + n_e\vec{\nabla}\bullet\vec{V} = \nabla\bullet D\nabla n_e + S_{ion} - S_{rec} \qquad (1)$$

The ionization and recombination of each charge state are computed within the KPRAD subroutines and summed to produce the final terms in equation (1). Whereas, quasi-neutrality is normally maintained with the assumption $n_e=n_i$, we now maintain the relationship $n_e=n_i+n_z\langle Z\rangle$, where n_z is the total impurity density and $\langle Z\rangle$ is the impurity average charge. Thus n_i is a dependent variable determined by its relationship to the other three. However, the present version has only one continuity equation, and the impurity ions are pushed along with the electrons so as to maintain an approximately constant impurity fraction over a localized region of the grid. The momentum equation and Ohm's law are unchanged except for the incorporation of the impurity contribution to the mass density and pressure, and the inclusion of Z_{eff} dependence in the resistivity, where Z_{eff} is now computed locally. The temperature equation contains an additional sink term which includes the total radiated power density calculated within the KPRAD subroutines and adiabatic cooling.

$$n_e \frac{dT_e}{dt} = (\gamma - 1)[n_e T_e \vec{\nabla} \cdot \vec{V} + \vec{\nabla} \cdot \vec{q}_e - Q_{loss}] \quad (2)$$

Ohmic heating is also accounted for in the final term of equation (2).

4. Initial Tests of NIMRAD

The initial penetration of the gas jet to just a few cm past the separatrix has been simulated at true experimental parameters ($S \sim 10^7$) as a test of both the ablation pressure penetration model and the KPRAD subroutines. The gas jet problem involves several independent time scales, related to resistive diffusion, radiation, and thermal conduction, as well as the gas sound speed. For instance, the interaction between radiation and Ohmic heating affects the jet penetration speed, as does the perpendicular thermal conductivity. Thus, the first experimental comparison is done with all parameters set to experimental values to avoid uncertainties about scaling and assess the accuracy of the model.

Density profiles from simulations of helium and argon jet penetration are shown in FIG. 6. Significant differences are observed as each species interacts with the plasma. The helium gas jet ionizes heavily and produces a large density spike ($>10^{21}$ m^{-3}) which propagates inward with the jet. Near the separatrix, as the edge becomes very cool, the density falls back to approximately target levels. Because it radiates more efficiently, the argon gas jet cools the plasma much more quickly, and consequently becomes substantially less ionized. A small density spike is present at the jet leading edge, but a density drop below target levels occurs in its wake due to deuterium 3-body recombination. Each of these features is commonly observed in Alcator C-Mod experiments, as seen in the Thomson scattering profiles in FIG. 6.

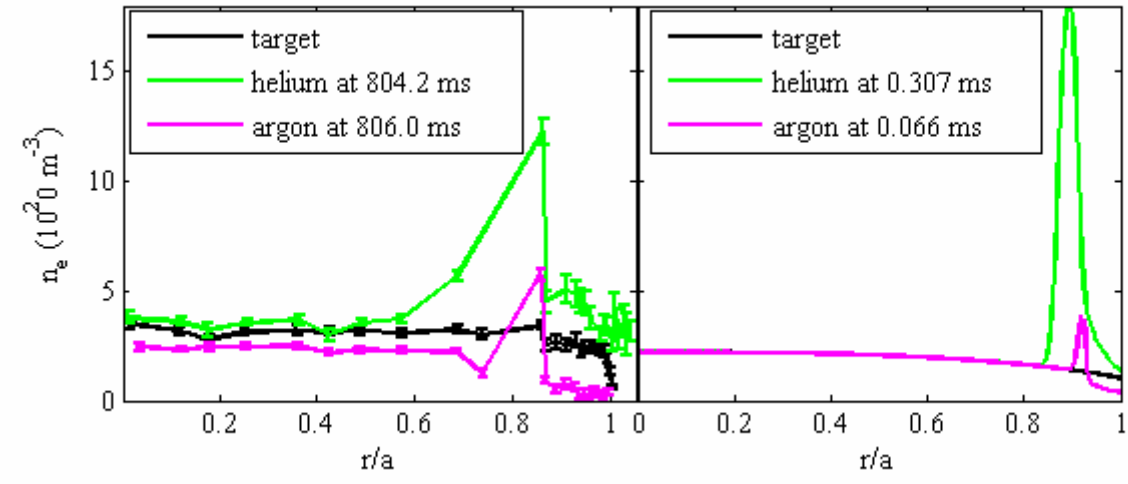

FIG. 6. (left) Thomson scattering profiles from C-Mod showing the target density profile and profiles taken during separate helium (1050811005) and argon (1050722016) gas jet shots. In both cases the gas jet is fired at 800 ms and takes several ms to reach the plasma edge, varying with sound speed. The profiles show the early interaction of the jet with the plasma, but the times are not meant to correspond precisely with those of the simulated profiles. (right) Density profiles from the NIMRAD simulations with helium and argon, exhibiting the features commonly observed in C-Mod experiments with each gas.

Because of the stronger radiation, much faster penetration of the neutral argon jet occurs as expected from the ablation pressure model. Gigawatt levels of radiated power are required to quench C-Mod on the ms experimental time scales observed. In a lower S argon simulation, total radiated power is seen to rise to over 1 GW (FIG. 7) as MHD modes become large enough to destroy closed flux surfaces, allowing rapid heat transport into the high impurity region.

Simulations of helium, neon, and argon gas jets can be carried out at reduced S with radiation and transport times scaled along with the L/R time to allow computationally efficient simulations of the entire thermal quench and direct comparison with C-Mod data.

5. Summary

MHD simulations have successfully captured the major qualitative features of gas jet mitigation experiments on Alcator C-Mod, shedding light on the mechanism by which a shallow penetrating gas jet induces a core thermal quench. However, several experimental observations, such as the differences between low and high-Z impurity penetration and mixing, can not be reproduced in the simulations without a more sophisticated gas jet model. The atomic physics code KPRAD has been incorporated into NIMROD to allow detailed simulations of the interaction between the tokamak plasma and the gas jet. Tests of the combined code are able to reproduce some differences observed between helium and argon gas jets. All physics included in the code is derived from first principles; thus, successful benchmarking against Alcator C-Mod and other present tokamaks should allow confident extrapolation to ITER. Both Thomson scattering and bolometry data will play an important role in the benchmarking process.

Several upgrades for the NIMRAD code are planned. These include localization of the jet and the addition of a continuity equation for the impurities. Once the computational domain is extended beyond the separatrix to the first wall, predictions for both heat deposition and halo

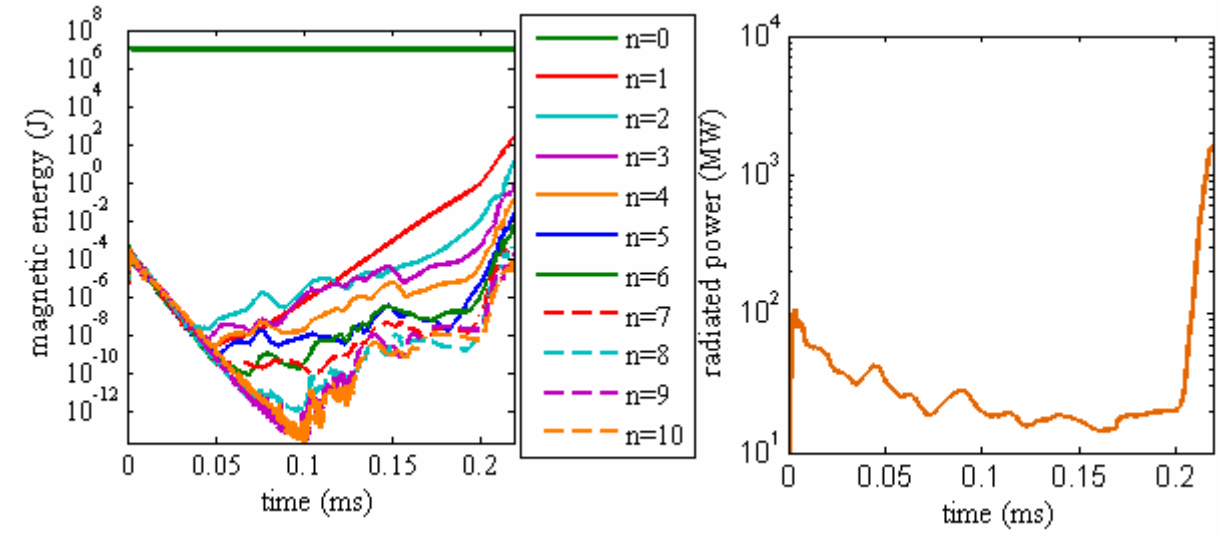

FIG. 7. (left) Magnetic energy spectrum for an argon simulation with $S=10^4$. MHD modes become sufficiently large to destroy closed flux surfaces at around 0.2 ms. (right) Total radiated power for the argon has jet simulation. Jump to ~1 GW at 0.2 ms is precipitated by destruction of closed flux surfaces.

currents will be possible. Density, electric field and magnetic fluctuation data can be analyzed in post processing to predict runaway current generation. An optimum strategy for mitigating each of these effects can then be devised.

---

[1] D.G. Whyte, *et. al*., *Phys. Rev. Lett.*, **89** (2002) 055001.
[2] D.G. Whyte, *et. al*., *J. Nucl. Mater.* **313-316** (2003) 1293.
[3] E.M. Hollman, *et. al*., in Fusion Energy 2004 (Proc. 20th Int. Conf. Vilamoura, 2004) (Vienna: IAEA) CD-ROM file EX/10-6Ra; online publication available from Spring 2005.
[4] R. Granetz, *et. al.*, "Gas Jet Disruption Mitigation Studies on Alcator C-Mod", submitted to *Nuclear Fusion.*
[5] V.A. Izzo, *Nuclear Fusion* **46** (2006) 541.
[6] D.G. Whyte, in *Proc. 24th European Conference on Controlled Fusion and Plasma Physics*, Berchtesgaden, Germany, 1997, Vol. 21A, p. 1137.
[7] P.B. Parks, *et. al., Fusion Technology*, **35** (1999) 267.